arXiv:1406.7070v1 [cond-mat.stat-mech] 27 Jun 2014

High-precision Estimate of the Critical Exponents for the Directed Ising Universality Class

Su-Chan Park*
Department of Physics, The Catholic University of Korea, Bucheon 420-743, Republic of Korea

With extensive Monte Carlo simulations, we present high-precision estimates of the critical exponents of branching annihilating random walks with two offspring, a prototypical model of the directed Ising universality class in one dimension. To estimate the exponents accurately, we propose a systematic method to find corrections to scaling whose leading behavior is supposed to take the form $t^{-\chi}$ in the long-time limit at the critical point. Our study shows that $\chi \approx 0.75$ for the number of particles in defect simulations and $\chi \approx 0.5$ for other measured quantities, which should be compared with the widely used value of $\chi = 1$. Using χ so obtained, we analyze the effective exponents to find that $\beta/\nu_\parallel = 0.2872(2)$, $z = 1.7415(5)$, $\eta = 0.0000(2)$, and accordingly, $\beta/\nu_\perp = 0.5000(6)$. Our numerical results for $\beta/\nu_\parallel$ and z are clearly different from the conjectured rational numbers $\beta/\nu_\parallel = \frac{2}{7} \approx 0.2857$, $z = \frac{7}{4} = 1.75$ by Jensen [Phys. Rev. E, **50**, 3623 (1994)]. Our result for $\beta/\nu_\perp$, however, is consistent with $\frac{1}{2}$, which is believed to be exact.

PACS numbers: 64.60.Ht, 05.70.Ln, 05.10.-a
Keywords: High-precision estimate, Critical exponents, Corrections to scaling, Directed Ising universality class

I. INTRODUCTION

Absorbing phase transitions have been extensively studied during the last several decades. Just like equilibrium systems, these non-equilibrium systems are categorized by several universality classes according to symmetry and conservation. Notable examples are the directed percolation (DP) class and the directed Ising (DI) class, to name only a few (for an exhaustive review on universality classes, see, e.g., Refs. [1] and [2]).

Although the deciding features of these universality classes are quite well, if not completely, understood (see, for instance, Refs. [1] and [2] and references therein), an exact solution of a typical model, even in one dimension, is still not available. The importance of exact solutions for understanding physical systems in theoretical physics cannot be exaggerated, and an ample example is the Onsager solution of the two-dimensional Ising model [3]. By the same token, any exact solution of a model belonging to DP or DI class is still desired.

Since exact solvability is intimately related to critical exponents' being rational numbers, whether the critical exponents obtained from numerical studies can be represented by rational numbers has always been a question. For the DP class in one dimension, a certain set of rational numbers was proposed as the critical exponents, but later a detailed numerical analysis clearly disproved that conjecture [4]. On that account, it does not seem that an exact solution can be found for the DP class. For the DI universality class, a set of rational numbers for critical exponents was also conjectured [5]. Although numerical results in the literature look consistent with the conjectured values within error bars, whether this conjecture is true or not remains unanswered.

The main aim of this paper is two fold. First, we would like to draw a firm conclusion as to whether the critical exponents for the DI class in one dimension are rational numbers. To state the conclusion first, our extensive numerical study disproves the conjecture by Jensen [5]. Second, we suggest a numerical method to extract corrections to scaling that are important for accurate estimates of the critical exponents. As we will see later, information as to how corrections to scaling behave at the critical point is crucial when it comes to estimating the critical exponents accurately.

This paper is organized as follows: Section II introduces a model and defines the quantities in which we are interested. In Sec. III, we propose a numerical method to find corrections to scaling from Monte Carlo simulation data. Using this method in Sec. IV, we find the critical exponents by studying the corresponding effective exponents. We summarize our results in Sec. V.

II. MODEL

We consider a one-dimensional branching annihilating random walk with two offspring (BAW2), which is a prototypical model belonging to the DI class in one dimension. Among many versions of the BAW2, we chose the model introduced in Ref. [6]. For completeness, we explain below the model and the algorithm we used for the simulations.

The BAW2 is defined on a one-dimensional lattice of size L with periodic boundary conditions. Each lattice site can be either occupied by a particle (A) or be vacant ($\emptyset$). Double occupancy is not allowed. Each particle can hop to one of its nearest neighbors or can branch two

*Electronic address: spark0@catholic.ac.kr; Fax: +82-2-2164-4764

offspring. The detailed dynamic rules are as follows:

$$A\emptyset \xleftrightarrow{(1-p)/2} \emptyset A, \quad AA \xrightarrow{(1-p)q} \emptyset\emptyset,$$
$$\emptyset A\emptyset \xrightarrow{p} AAA, \quad AAA \xrightarrow{pq} \emptyset A\emptyset, \quad AA\emptyset \xleftrightarrow{pq} \emptyset AA, \quad (1)$$

where the parameters over the arrows represent the corresponding transition rates.

When $q = 1$, this model is exactly solvable [7] but it does not have a nontrivial phase transition in the sense that for any $p < 1$, the density decays to zero as $t^{-1/2}$ with time t. Only when q is smaller than 1, there is a nontrivial critical point $p_c < 1$, and the model belongs to the DI class. In this paper, we fix $q = 0.5$ (as in Ref. [6]) and investigate the behavior of the BAW2 as p varies around the critical point p_c. When $p < p_c$ ($p > p_c$), the system is said to be in the absorbing (active) phase.

In simulations, we used the following algorithm. Assume that there are $N(t)$ particles at time t in the system. Among the $N(t)$ particles, a particle is chosen at random. It may hop to one of its neighbors (with probability $1 - p$) or may branch two offspring to its two nearest neighbors (with probability p). If a branching attempt is tried with probability p, its two neighbors (to be called target sites) are examined. If both target sites are empty, these two sites become occupied with probability 1. If one or both of the target sites are already occupied, the branching attempt becomes successful only with probability q, but with probability $1-q$ this branching attempt is ignored, and nothing happens. Assume that the branching attempt turns out to be successful. The empty target site becomes occupied, but the occupied target site becomes empty because of an immediate pair-annihilation event of new and occupied particles. In hopping attempts, one of two possible directions (left or right) is selected at random. If the selected site is vacant, it lands there with probability 1. If the selected site is occupied, the two particles undergo pair-annihilation with probability q, but the hopping can be ignored with probability $1 - q$, and nothing happens. After an attempt described above, time increases by $1/N(t)$ regardless of whether the attempt changes the configuration or not. We repeat the above procedure until either the system loses all particles or time exceeds the preassigned maximum observation time $t_{\max}$.

In simulations, we used two kinds of initial conditions. In one case, simulations begin with the fully-occupied initial condition (FOIC); that is, $N(t = 0) = L$. In the literature, simulations starting from the FOIC are generally referred to as static simulations. We will also use this terminology in this paper. In the other case, all but a few sites in the middle are empty. If two consecutive sites are occupied ($N(0) = 2$), this initial condition will be called the two-particle initial condition (TPIC). We also simulated the stochastic evolution starting from a single particle in the whole system ($N(0) = 1$), which will be called the single-particle initial condition (SPIC). Simulations starting from either the TPIC or the SPIC will be referred to as defect simulations. In defect simulations, the system size L should be large enough so that no particle can hit the boundary up to $t_{\max}$ to ensure that the system size is effectively infinite.

In static simulations, we measured the density $\rho(t) = \langle N(t)\rangle/L$ and the survival probability $P(t) \equiv \langle 1 - \delta_{N(t),0}\rangle$, where $\langle \ldots \rangle$ means the average over all realizations and $\delta_{x,y}$ is the Kronecker delta symbol, which should not be confused with the critical exponent δ introduced later. We will also study the density averaged over surviving samples, $\rho_s(t)$, which is calculated as $\rho_s(t) = \rho(t)/P(t)$.

In defect simulations, we measured the average number of particles $n(t) \equiv \langle N(t)\rangle$, the survival probability $S(t) \equiv \langle 1 - \delta_{N(t),0}\rangle$, and the square of the distance between the two most distant particles averaged over surviving samples, $R^2(t)$. Note that we use different symbols for the survival probability depending on which simulation scheme (static or defect) is under consideration.

III. SCALING RELATION AND CORRECTIONS TO SCALING

According to the scaling theory (for a review, see, e. g., Refs. [1] and [2]), the asymptotic behavior of $n(t)$, $S(t)$, and $R^2(t)$ near the critical point p_c is described as

$$\begin{aligned} n(t) &\sim t^{\eta} f\left(\Delta t^{1/\nu_\parallel}\right), \\ S(t) &\sim t^{-\delta'} g\left(\Delta t^{1/\nu_\parallel}\right), \\ R^2(t) &\sim t^{2/z} h\left(\Delta t^{1/\nu_\parallel}\right), \end{aligned} \quad (2)$$

where $\Delta \equiv p - p_c$, f, g, and h are scaling functions that are not singular at the origin, and η, $\nu_\parallel$, δ', and z are critical exponents.

When the SPIC is used, $S(t) = 1$ for all t because of the modulo-2 conservation of the number of particles in the system. Obviously, $\delta' = 0$ in the case of the SPIC. In what follows, $S(t)$ exclusively means the survival probability of defect simulations with the TPIC. When the TPIC is used,

$$\lim_{t\to\infty} S(t) \sim \begin{cases} (p - p_c)^{\beta'}, & p > p_c \text{ (active phase)}, \\ 0, & p < p_c \text{ (absorbing phase)}, \end{cases} \quad (3)$$

which gives the scaling relation $\delta' = \beta'/\nu_\parallel$. Likewise, $\rho(t)$ and $\rho_s(t)$ are expected to behave as

$$\begin{aligned} \rho(t) &= t^{-\delta} f_r(t/L^z, \Delta t^{1/\nu_\parallel}), \\ \rho_s(t) &= t^{-\delta} g_r(t/L^z, \Delta t^{1/\nu_\parallel}), \end{aligned} \quad (4)$$

where δ is another critical exponent, and f_r and g_r are scaling functions. Since

$$\lim_{t\to\infty} \lim_{L\to\infty} \rho(t) \sim (p - p_c)^{\beta}, \quad (5)$$

for $p > p_c$, δ should be equal to $\beta/\nu_\parallel$. In general, β need not be equal to β', but the duality relation proven

in Ref. [8] implies that β should be equal to β' for the BAW2.

Also, there is the generalized hyperscaling relation [9]

$$\eta + \delta' + \delta = \frac{d}{z}, \tag{6}$$

where d is the dimensions in which the system is embedded (in this paper, d is always 1). Note that the above relation is insensitive to the initial conditions of the defect simulations, although η and δ' individually may be non-universal.

To estimate the critical exponents systematically, one generally uses the effective exponents defined as

$$\begin{aligned} \eta_{\rm eff}(t) &\equiv \ln\left(n(t)/n(t/b)\right)/\ln b, \\ -\delta'_{\rm eff}(t) &\equiv \ln\left(S(t)/S(t/b)\right)/\ln b, \\ \frac{2}{z_{\rm eff}(t)} &\equiv \ln\left(R^2(t)/R^2(t/b)\right)/\ln b, \\ -\delta_{\rm eff}(t) &\equiv \ln\left(\rho(t)/\rho(t/b)\right)/\ln b, \end{aligned} \tag{7}$$

where b is a constant (in this paper, we set $b = 10$). In general, there are corrections to scaling, and the measured quantities at the critical point are expected to behave as

$$\begin{aligned} n(t) &= a_n t^{\eta}\left(1 + c_n t^{-\chi_n} + o(t^{-\chi_R})\right), \\ S(t) &= a_s t^{-\delta'}\left(1 + c_s t^{-\chi_s} + o(t^{-\chi_s})\right), \\ R^2(t) &= a_r t^{2/z}\left(1 + c_r t^{-\chi_r} + o(t^{-\chi_r})\right), \\ \rho(t) &= a_\rho t^{-\delta}\left(1 + c_\rho t^{-\chi_\rho} + o(t^{-\chi_\rho})\right), \end{aligned} \tag{8}$$

where a's and c's are constants and χ's, which will be called the leading corrections to the scaling exponents (LCSEs), should be positive. Accordingly, the effective exponents at criticality become

$$\begin{aligned} \eta_{\rm eff}(t) &= \eta - \frac{c_n}{\ln b}(b^{\chi_n} - 1)t^{-\chi_n} + o(t^{-\chi_n}), \\ -\delta'_{\rm eff}(t) &= -\delta' - \frac{c_s}{\ln b}(b^{\chi_s} - 1)t^{-\chi_s} + o(t^{-\chi_s}), \\ \frac{2}{z_{\rm eff}(t)} &= \frac{2}{z} - \frac{c_r}{\ln b}(b^{\chi_r} - 1)t^{-\chi_r} + o(t^{-\chi_r}), \\ -\delta_{\rm eff}(t) &= -\delta - \frac{c_\rho}{\ln b}(b^{\chi_\rho} - 1)t^{-\chi_\rho} + o(t^{-\chi_\rho}). \end{aligned} \tag{9}$$

If we plot an effective exponent, for instance $\eta_{\rm eff}$, as a function of $t^{-\chi_n}$ with the correct value of χ_n, $\eta_{\rm eff}(t)$ should approach the y axis with finite slope at the critical point. Furthermore, if the system is in the active (absorbing) phase, effective exponents should eventually veer up (down) after following a straight line for some time region. Thus, if the goal of obtaining high-precision estimates of the critical exponents is to be achieved, correct information about the LCSE is indispensable.

For models belonging to the DI class, the LCSE is normally belived to be 1; for an example, see Eq. (5) of Ref. [5]. However, numerical data seem to suggest that corrections to scaling for certain quantities are stronger than expected. Hence, we feel it necessary to find the LCSE more systematically. To this end, we introduce the leading-correction-to-scaling function $\Theta_n(t)$ as

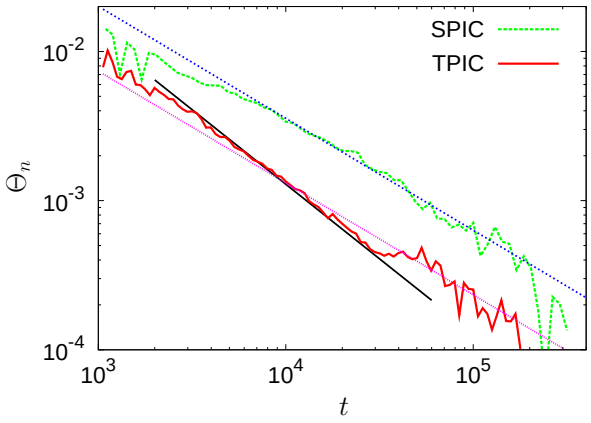

FIG. 1: (Color online) Log-log plots of $\Theta_{n1}(t)$ vs t (upper curve) and $\Theta_{n2}(t)$ vs t (lower curve) at $p = 0.494\ 675$. Straight lines with slopes of about -0.75 are resulting fitting functions for the corresponding curves. A line segment with a slope of -1 is also drawn for comparison.

$$\Theta_n(t) \equiv \left| \frac{n(t)n(t/b^2)}{n(t/b)^2} - 1 \right|. \tag{10}$$

In a similar fashion, we can define $\Theta_s(t)$, $\Theta_r(t)$, and $\Theta_\rho(t)$ for $S(t)$, $R^2(t)$, and $\rho(t)$, respectively. By a straightforward calculation using Eqs. (8) and (10), the long time behavior of $\Theta_n(t)$ at criticality becomes

$$\Theta_n(t) = |c_n|\left(b^{\chi_n} - 1\right)^2 t^{-\chi_s} + o(t^{-\chi_n}). \tag{11}$$

Thus, without prior knowledge of the critical exponents, we can estimate the LCSE by investigating the leading-correction-to-scaling function.

Although we do not know p_c *a priori* in most cases, the leading-correction-to-scaling functions and critical exponents, as well as p_c, are obtained at the same time by using the following iterative procedure: At first, we make a rough guess about the LCSE, for example, $\chi = 1$. Although the value of the LCSE can be wrong, one can manage to estimate the critical point with a certain error by observing how a plot of the effective exponent vs t^{-1} behaves. Now, we calculate the Θ function and estimate χ at the obtained critical point in the above step. Then, with the χ obtained from the Θ function, we re-estimate the critical point from longer-time simulations by analyzing plots of the effective exponents against $t^{-\chi}$. At this step, the accuracy of the critical point becomes improved, so we re-estimate χ by using the Θ function at the critical point. We repeat the above steps until the resulting values of the χ, p_c, and exponents become consistent with the scaling theory. In this paper, we only present the final result of the above procedure.

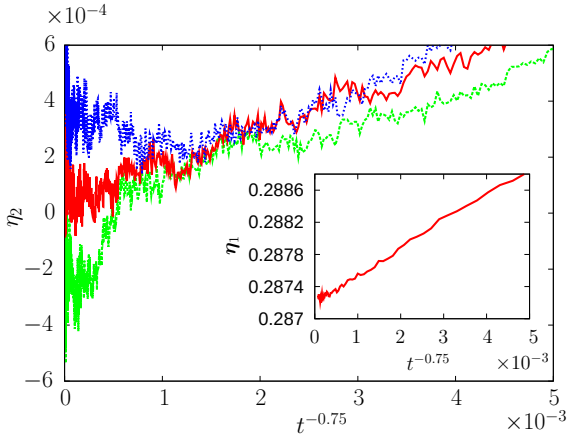

FIG. 2: (Color online) Plots of $\eta_2(t)$ vs $t^{-0.75}$ for $p = 0.4947$, 0.494 675, and 0.494 65 (top to bottom). Inset: Plot of $\eta_1(t)$ vs $t^{-0.75}$ at $p = 0.494\ 675$.

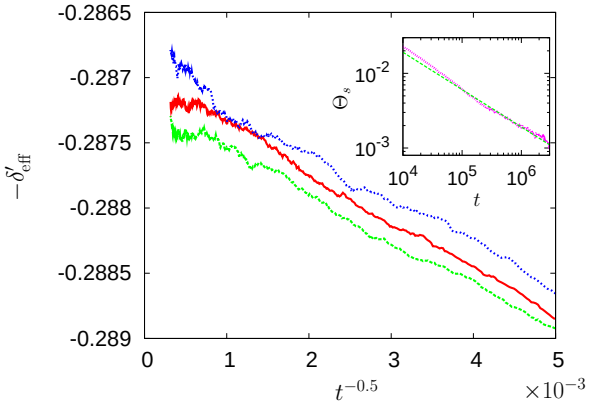

FIG. 3: (Color online) Plots of $-\delta_{\rm eff}(t)$ vs $t^{-0.5}$ for $p = 0.4947$, 0.494 675, and 0.494 65 (top to bottom). Inset: Plot of $\Theta_s(t)$ vs t at $p = 0.494\ 675$ on a double-logarithmic scale. The straight line whose slope is about -0.5 is the result of the fitting in the long-time region.

IV. SIMULATION RESULTS

This section presents simulations results. We begin with analyzing $\Theta_n(t)$ and $\eta_{\rm eff}$ from defect simulations with two different initial conditions. For convenience, $\eta_{\rm eff}$ obtained from the defect simulations with the SPIC (TPIC) will be denoted by η_1 (η_2). Likewise, Θ_n with the SPIC (TPIC) will be denoted by Θ_{n1} (Θ_{n2}).

At first, we will show how Θ_{n1} and Θ_{n2} behave at $p = 0.494\ 675$, which we claim to be the critical point of the model. Θ_{n1} (Θ_{n2}) is obtained from 2×10^8 (1.5×10^{10}) independent runs up to $t_{\rm max} = 10^{5.5}$ with $b = 10$, but our data for $t > 2 \times 10^5$ are too noisy to get reliable information. Figure 1 shows double logarithmic plots of $\Theta_{n1}(t)$ and $\Theta_{n2}(t)$ against t. Both functions are well fitted by a power-law function $Ct^{-\chi_n}$ with $\chi_n \approx 0.75$ in the long-time limit and with $C \approx 3.0$ (1.3) when using the SPIC (TPIC) (see the two straight lines in Fig. 1). Notice that $\Theta_{n2}(t)$ is initially well fitted by t^{-1} (see the line segment with a slope of -1 in Fig. 1), which might be the reason the effective exponents plotted against t^{-1} in the literature have given plausible results.

Figure 2 depicts η_2 against $t^{-0.75}$ for $p = 0.494\ 65$, 0.494 675, and 0.4947 (bottom to top), and the inset of Fig. 2 shows the behavior of η_1 plotted against $t^{-0.75}$ at $p = 0.494\ 675$. For η_1, we used the same simulation results that were used to calculate Θ_{n1} in Fig. 1, but for η_2, we performed other simulations up to $t_{\rm max} = 10^7$ with the TPIC. In this case, the number of independent runs for $p = 0.494\ 65$, 0.494 675, and 0.4947 were 8×10^8, 8×10^8, and 5×10^8, respectively. At $p = 0.494\ 675$, η_2 becomes a straight line in the region where $t^{-0.75} \le 4\times10^{-3}$, but the curve for $p = 0.4947$ (0.494 65) veers up (down). Thus, we conclude that for the TPIC, $p_c = 0.494\ 675(25)$ and $\eta = 0.0000(2)$, where numbers in parentheses indicate the errors of the last digits. Note that our estimate of the critical point is more accurate than that given in Ref. [6]. The defect simulation with the SPIC at p_c gives $\eta_1 = 0.2872(1)$.

Now, we will move to the effective exponent $\delta'_{\rm eff}$. In Fig. 3, we depict $-\delta'_{\rm eff}(t)$ as a function of $t^{-0.5}$ for $p = 0.4947$, 0.494 675, and 0.494 65. Because, as shown in the inset of Fig. 3, $\Theta_s(t)$ behaves as $\sim t^{-0.5}$ in the long-time limit, we plot $-\delta'_{\rm eff}$ against $t^{-0.5}$. By extrapolating $-\delta'_{\rm eff}$ for $p = p_c$, we get $\delta' = 0.2872(2)$. Notice that the corrections to scaling for $S(t)$ are stronger than that for $n(t)$.

Finally, we will present the analysis of z. It turns out that the data for R^2 are the noisiest among the measured quantities, so it is very hard to see a clean asymptotic behavior of Θ_r. Nevertheless we will argue that χ_r, the LCSE for R^2, is equal to χ_s. First note that according to the duality relation [8], $\rho(t)$ from static simulations and $S(t)$ with the TPIC should behave in the same way. Thus, the LCSE for $\rho(t)$, that is, χ_ρ, should be equal to

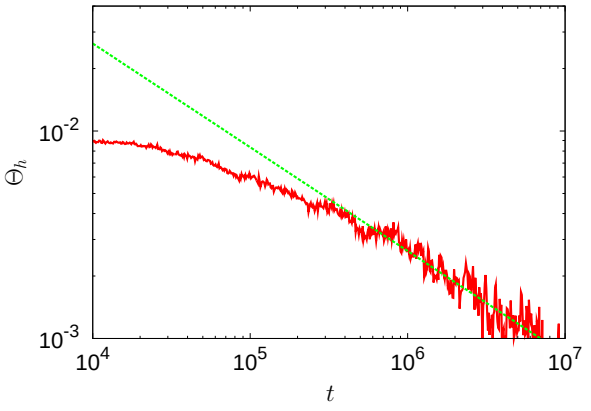

FIG. 4: (Color online) Double-logarithmic plot of Θ_h vs t for $p = 0.494\ 675$. The straight line with a slope of -0.5 is also drawn as a guide for the eyes.

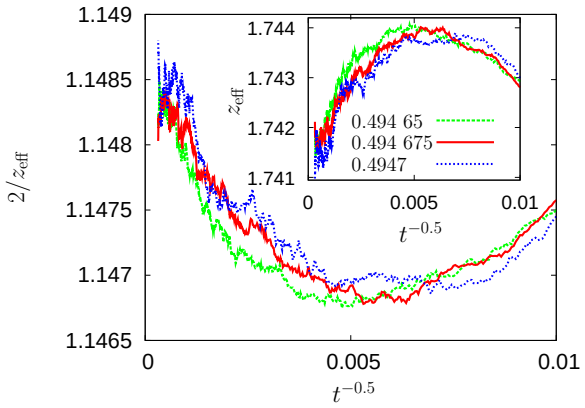

FIG. 5: (Color online) Plots of $2/z_{\rm eff}$ vs $t^{-0.5}$ for $p = 0.4947$, 0.494 675, and 0.494 65. Inset: Plots of $z_{\rm eff}$ vs $t^{-0.5}$ for the same set of p's. $z_{\rm eff}$ is defined as $2/(2/z_{\rm eff})$.

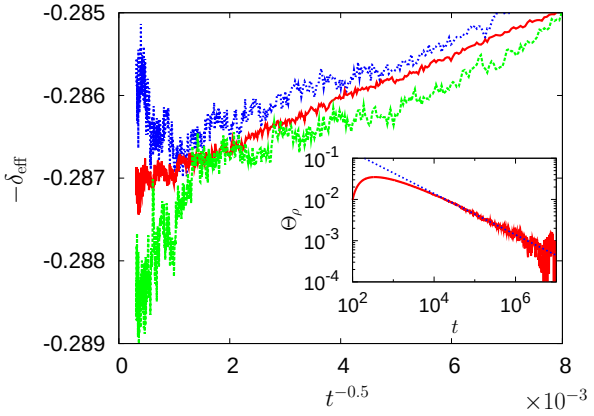

FIG. 6: (Color online) Effective exponents $-\delta_{\rm eff}$ for $p = 0.494\ 75$, 0.494 675, and 0.4946 (top to bottom) as functions of $t^{-0.5}$. Inset: Log-log plot of Θ_ρ against t at p_c. The straight line with a slope of about -0.5 is the resulting fitting function of the long-time behavior.

χ_s. Also, according to the hyperscaling relations that are derived by using the relation

$$\rho(t) \sim \frac{n(t)}{S(t)\sqrt{R^2(t)}}, \tag{12}$$

both sides of Eq. (12) are expected to have the same strengths of corrections to scaling. In Fig. 4, we depict a double-logarithmic plot of $\Theta_h(t)$ against t, where

$$\begin{aligned} \Theta_h &\equiv \frac{H(t)H(t/b^2)}{H(t/b)^2} - 1, \\ H(t) &\equiv \frac{n(t)}{S(t)\sqrt{R^2(t)}}. \end{aligned} \tag{13}$$

Indeed, this function shows a $t^{-0.5}$ behavior in the long-time limit. Thus, χ_r should not be smaller than $\chi_s = \chi_\rho$. Hence, $\chi_r \geq \chi_s$ should be satisfied. On the other hand, $R^2(t)$ seems to have stronger corrections to scaling than $S(t)$, which implies $\chi_r \leq \chi_s$. Hence, χ_r should be equal to χ_s.

In Fig. 5, we plot $2/z_{\rm eff}$ against $t^{-0.5}$ near criticality. From this figure, we conclude that $2/z = 1.1484(4)$ or $z = 1.7415(5)$. See the inset of Fig. 5, which depicts the behavior of $z_{\rm eff} \equiv 2/(2/z_{\rm eff})$.

Next, we will present the results of static simulations. At first, we analyze $\delta_{\rm eff}$ near criticality, as well as the correction-to-scaling function Θ_ρ at the critical point. In Fig. 6, we show the behavior of $\delta_{\rm eff}$ near criticality. These curves are obtained from simulations with size $L = 2^{23}$ for the maximum observation time $t_{\rm max} = 10^7$ at $p = 0.494\ 75$ (2400 runs), 0.494 675 (10 000 runs), and 0.4946 (2400 runs) from top to bottom. Up to $t_{\rm max}$, no sample run has fallen into the absorbing state, which minimally supports the finite size effect not being significant. Later, we will affirm this statement from a finite-size scaling analysis. The inset of Fig. 6 gives the reason $-\delta_{\rm eff}$ is plotted against $t^{-0.5}$; in the long-time limit, Θ_ρ decays as $t^{-0.5}$ at $p = p_c$. Hence, we conclude that $\delta = 0.2872(1)$, which is consistent with the duality relation $\delta = \delta'$. Also, note that within the error bars, our exponents are consistent with the hyperscaling relation Eq. (6). In particular, if η_2 is exactly 0 (see Fig. 2), we see that $2\delta = 1/z$ or $\delta z \equiv \beta/\nu_\perp = \frac{1}{2}$, exactly.

Figure 7 depicts the finite-size scaling collapse at the critical point. According to the scaling ansatz in Eq. (4), plots of $\rho(t)t^\delta$ vs t/L^z for different L's at the critical point should collapse into a single curve. Indeed, this scaling collapse is clearly observed in Fig. 7 when we use the critical exponents obtained above. Also, the inset of Fig. 7 clearly shows the scaling collapse of plots of $\rho_s(t)L^{0.5}$ vs t/L^z, which is consistent with $\beta/\nu_\perp = \frac{1}{2}$, obtained from the hyperscaling relation. Because the finite-size effect becomes significant when $t \geq 0.1 \times L^z$, as can be deduced from Fig. 7, we expect the finite-size effect for $L = 2^{23}$

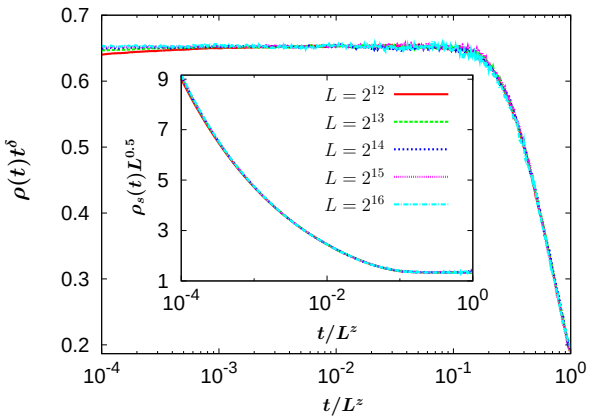

FIG. 7: (Color online) Scaling collapse plots of $\rho(t)t^\delta$ vs t/L^z with $\delta = 0.2872$ and $z = 1.7415$ for $L = 2^{12}$, 2^{13}, 2^{14}, 2^{15}, and 2^{16} at $p = p_c$ on a semi-logarithmic scale. Inset: Scaling collapse plots of $\rho_s(t)L^{0.5}$ vs t/L^z for the same system sizes at criticality on a semi-logarithmic scale.

TABLE I: Critical exponents of the BAW2 in one dimension.

exponents	simulations	conjecture [5]
η	0.0000(2)	0
$\beta/\nu_\parallel$	0.2872(2)	$\frac{2}{7} \approx 0.2857$
z	1.7415(5)	$\frac{7}{4}$
$\beta/\nu_\perp$	0.5000(6)	$\frac{1}{2}$

to become crucial when $t \geq 10^{12}$, which is much larger than the maximum observation time 10^7 in Fig. 6. Thus, we did not have to take the finite-size effect into account when we analyzed $\delta_{\rm eff}$ in Fig. 6.

V. SUMMARY

To sum up, we presented high-precision estimates of the critical exponents for the branching annihilating random walks with two offspring, which is a prototypical model belonging to the directed Ising universality class in one dimension. To this end, we first analyzed corrections to scaling by using the correction-to-scaling functions defined in Eq. (10). This method can be easily applicable to any critical systems, although reducing statistical fluctuations by simulating many independent runs is the main practical obstacle. From this analysis, we found that the LCSE for $n(t)$ was about 0.75, but those for other measured quantities were all around 0.5. With the LCSE obtained, we analyzed the effective exponents and found that $\eta = 0.0000(2)$ and $\delta' = 0.2872(2)$ when the two-particle initial condition was used and that $\eta = 0.2872(1)$ and $\delta' = 0$ when the single-particle initial condition was used. We also found that $z = 1.7415(5)$ and $\delta = 0.2872(1)$. These exponents distinctively differ from the conjectured rational numbers $z = \frac{7}{4} = 1.75$ and $\delta = \frac{2}{7} \approx 0.2857$ in Ref. [5]. If η is exactly zero, the generalized hyperscaling relation, along with the duality property of the BAW2, shows that $\beta/\nu_\perp = \frac{1}{2}$ exactly, and our numerical simulations are consistent with this value within the error bars. All the numerical results are summarized in Table I, along with the conjectured values for comparison.

Acknowledgments

This work was supported by the Catholic University of Korea, Research Fund 2011 and by the Basic Science Research Program through the National Research Foundation of Korea (NRF) funded by the Ministry of Education, Science and Technology (Grant No. 2011-0014680).

[1] H. Hinrichsen, Adv. Phys. **49**, 815 (2000).
[2] G. Ódor, Rev. Mod. Phys. **76**, 663 (2004).
[3] L. Onsager, Phys. Rev. **65**, 117 (1944).
[4] I. Jensen, J. Phys. A **29**, 7013 (1996).
[5] I. Jensen, Phys. Rev. E **50**, 3623 (1994).
[6] D. Zhong and D. ben-Avraham, Phys. Lett. A **209**, 333 (1995).
[7] D. ben-Avraham, F. Leyvraz, and S. Redner, Phys. Rev. E **50**, 1843 (1994).
[8] K. Mussawisade, J. E. Santos, and G. M. Schütz, J. Phys. A **31**, 4381 (1998).
[9] J. F. F. Mendes, R. Dickman, M. Henkel, and M. C. Marques, J. Phys. A **27**, 3019 (1994).